T.1: Plasmonic nanoparticles synthesized using pulsed laser ablation and their optical properties

B. Tirumala Rao, S. Verma and L. M. Kukreja

Laser Materials Processing Division
E mail: trao@rrat.gov.in

1. Introduction: Plasmonic materials essentially show optical responses manifested by the collective oscillation of free electrons such as in metals also known as localized surface plasmon resonance (LSPR). Recently plasmonic metal nanoparticles (PMNPs) have received great interest because of their strong optical scattering and absorption along with enhanced near field as well as localized heating. Utilizing the aforesaid effects of PMNPs, many promising applications are emerging in the field of lasers, optoelectronics, light harvesting at nano-scale, molecular level sensing, imaging etc [1-3]. For an ellipsoidal metal nanoparticle (with radii a_1, a_2 and a_3) surrounded by a medium of dielectric constant ε_m, when interacting with light, under dipole approximation the induced polarizibilty is given by:

$$\alpha = 4\pi a_1 a_2 a_3 \frac{\varepsilon(\omega) - \varepsilon_m}{3\varepsilon_m + 3L[\varepsilon(\omega) - \varepsilon_m]}$$

where, $\varepsilon(\omega)$ is the frequency ω dependent dielectric function of the metal, and L is the geometrical factor (1/3 for sphere). Corresponding to this, the LSPR wavelength (frequency) of a spherical nanoparticle is predicted by the Frohlic condition, $Re[\varepsilon(\omega)] \approx \varepsilon_m(L-1)/L$. This shows that the LSPR response of the PMNPs is dependent on both intrinsic parameters like dielectric function of the metal and the extrinsic parameters like size, shape and also their spatial distribution (due to inter-particle interaction) along with surrounding dielectric medium. Because of these reasons, synthesis of PMNPs with controlled LSPR characteristics has become important for their effective utilization in a specific application. Laser being a non-contact, short duration, high intensity, localized heat source, capable to produce efficient and congruent ablation of materials either in vacuum or in different liquids shows potential for synthesis of PMNPs. Pulsed laser deposition (PLD) method offers single step growth of either nanoparticles or continuous films of variety of materials including metals, dielectrics and semiconductors or their composites with monolayer accuracy as required for the contemporary problems related to the field of plasmonics. In view of this, we initiated research on synthesis of PMNPs films as well as their colloidal dispersion in liquids using pulsed laser ablation based methods and studied their optical properties.

This article presents an overview of our recent research work on synthesis of PMNPs films supported on substrates and colloidal dispersions in different solutions using pulsed laser ablation and studies on their optical responses. The role of different process parameters mainly substrate temperature, number of pulses, target to substrate distance (TSD), dielectric capping layer etc on the morphology and LSPR response of mainly Au and Ag metals has been presented. Using sequential laser ablation of different metal targets, growth of LSPR wavelength tunable plasmonic alloy nanoparticles films of desired composition has been demonstrated. Theoretical calculations for dielectric functions of alloy nanoparticles and LSPR wavelengths of the densely packed PMNPs films using effective medium models including particle-substrate and particle-particle interactions are presented. Also in liquid-phase pulsed laser ablation (LPPLA) method, the effect of different process parameters such as ablation time, laser wavelength, type of liquid medium, pH of the liquid on LSPR and morphological properties of the PMNPs are discussed.

2. Growth of plasmonic nanoparticle films using PLD

Using KrF excimer laser (wavelength 248 nm, 20 ns pulse duration and 10 Hz repetition rate) Au, Ag and their alloy nanoparticle as well as continuous thin films were grown by PLD technique (Fig. T.1.1). The role of different process parameters on the morphology and LSPR responses of the PMNPs films studied using atomic force microscopy (AFM) and UV-VIS transmittance are presented in the following sections.

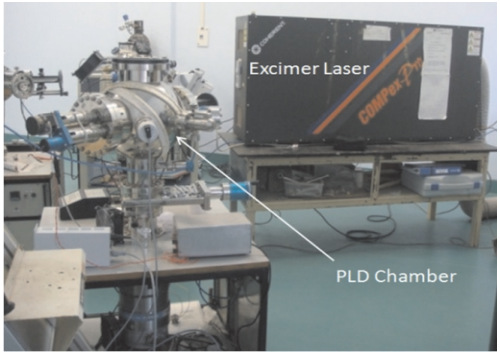

Fig. T.1.1: Experimental setup of pulsed laser deposition at our laboratory

2.1. Morphological characteristics

PLD is one of the physical vapor deposition methods where the high intensity laser pulses ablate the target material and thus formed plume reaches the substrate in highly directional manner. As a result of this, the film thickness and also its uniformity strongly depend on the substrate to target distance [4]. Fig. T.1.2 compares the morphology of Au films grown at 300˚C with 2500 number of pulses at 4.5, 6 and 7.5 cm TSD respectively. In all the cases, the formed PMNPs

were densely packed and their average size decreased with increasing the TSD. This is because, during initial stage of film growth, the nucleation density is proportional to the ratio of atomic flux received at the substrate and surface diffusion coefficient of adatoms. With increasing deposition, the nucleation sites grow and also coalesce with the adjacent particles resulting into decreased particle densities. At higher TSD, because of reduced atomic flux, the amount of Au deposition and coalescence of islands is expected to be low as a result, the particles were smaller in size and more in number as compared to those produced at low TSD. Thus for a given number of pulses, increase in TSD has noticeable effect on decreasing the mean size of the particle and also their size distribution.

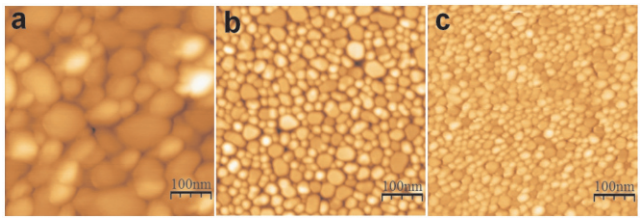

Fig. T.1.2: AFM images of Au nanoparticle films grown at TSD: 4.5 cm (a), 6.0 cm (b) and 7.5 cm (c).

At a given TSD, the film thickness can also be varied from number of ablation pulses. Fig. T.1.3 compares the morphology of the films with increasing number of ablation pulses where the mean size of the particles increased along with decrease in particle density.

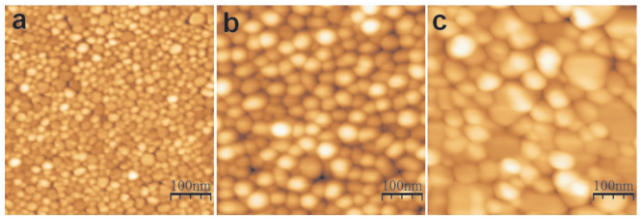

Fig. T.1.3: AFM images of Au nanoparticle films grown at TSD: 7.5 cm with number of pulses: 2500 (a), 5000 (b) and 7500 (c).

These results have demonstrated that the morphology of the nanoparticles can be controlled from the deposition atomic flux and also film mass thickness. On the other hand, for a given mass thickness of the film, the nucleation density and consequently the film's morphology can be controlled by altering the adatoms diffusion coefficient through the substrate growth temperature. The AFM images of Au films deposited with 5000 ablation pulses at varying substrate temperatures: room temperature (RT), 150˚C, 300˚C and 500˚C are shown in Fig. T.1.4 (a-d) [5]. The figure depicts significant variation in morphology of the films with growth temperature, the RT grown film showed interconnected nanoparticles of very small size with average height of about 1 nm. With increasing substrate temperature, the average size and also the average height of nanoparticles increased. At RT due to very low diffusivity of the adatoms, the film growth begins with high nucleation density and as deposition continues these growing clusters/nanoparticles quickly coalesce to form continuous films at relatively low mass thicknesses of about 5 nm [5]. On the other hand at high substrate temperatures, the particles grow with low nucleation density thereby resulted into nanoparticles films. For these films, about 300°C temperature was found to be optimum for formation of relatively uniform nanoparticles exhibiting narrow LSPR band as shown in the next section.

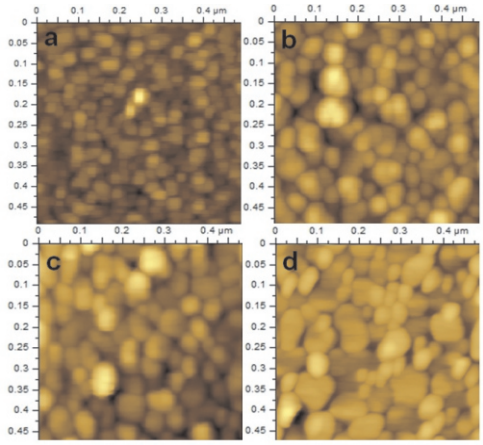

Fig. T.1.4: AFM images of Au nanoparticle films grown at substrate temperature: RT (a), 150 ºC (b), 300 ºC (c) and 500 ºC (d).

Other than monometallic PMNPs films, Ag-Au alloy nanoparticle films were also grown in a single step using sequential laser ablation of the two metal targets.

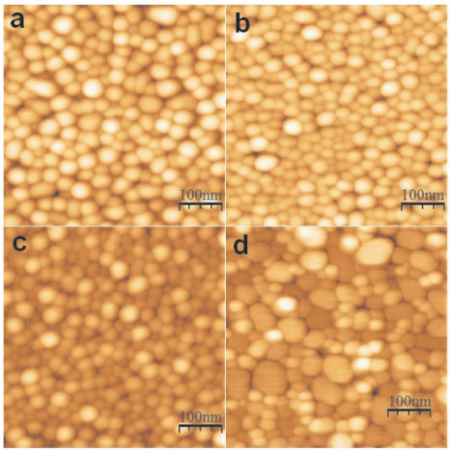

Fig. T.1.5: AFM images of Ag-Au alloy nanoparticle films with Ag:Au pulses ratio: 1:0 (a), 4:1 (b), 1:4 (c) and 0:1 (d).

Fig. T.1.5(a-d) presents the AFM images of the nanoparticle films grown with 4000 total number of pulses at 300ºC substrate temperature and different ratio of laser ablation pulses of Ag and Au as 1:0, 4:1, 1:4 and 0:1 respectively [6]. For the same film mass thickness, the monometallic films were formed with relatively larger average sizes and consequently lower particle densities compared to the alloy films. The height analysis of AFM micrographs showed the average height of about 12 nm for Ag nanoparticles film and 8 nm for pure Au film. Corresponding to this, the aspect ratio (diameter/height) of nanoparticles was found to be about 2.4 and 3.8 for Ag and Au films respectively.

2.2 LSPR characteristics

The effect of varying morphologies and compositions grown under different process parameters on the LSPR response of the films was analysed from optical transmission spectra. Fig.T.1.6 shows the transmission spectra of Au nanoparticle films grown at three different TSDs i.e. 4.5, 6 and 7.5 cm with 2500 number of ablation pulses (Fig.T.1.2). The LSPR responses of these films can be seen as significant dip in the transmission spectra with varying spectral widths depending on the morphology of the films at different TSDs. The figure shows that with decreasing TSD, the LSPR wavelength was red shifted and also broadened due to formation of larger and more irregular nanoparticles as seen from Fig.T.1.2. Also for the present case of supported nanoparticles films, the LSPR wavelength is significantly red-shifted with respect to those dispersed in liquid phase. It is because when nanoparticles are grown on substrates, their shape depends on substrate-film wetting properties and also the LSPR response is strongly influenced by different interactions like particle-particle and particle-substrate as discussed in theoretical section.

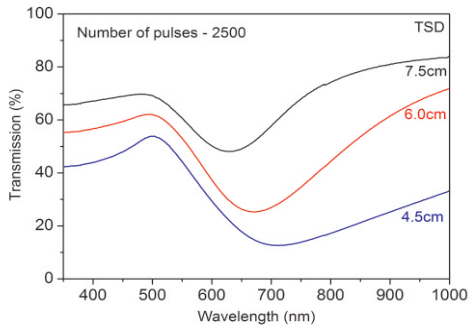

Fig. T.1.6: Optical transmission spectra of the Au films grown at different TSDs

Fig. T.1.7 presents the optical transmission spectra of Au nanoparticle films grown with different numbers of laser ablation pulses i.e. 2500, 5000 and 7500 at 300°C substrate temperature. With increasing number of laser ablation pulses, the LSPR wavelength was continuously red-shifted and also broadened. Different mechanisms like surface scattering, interface damping contribute to homogeneous broadening which depend inversely on particle size and dispersion in particles' size and shape give rise to inhomogeneous broadening. The observed increased broadening with number of pulses is mostly inhomogeneous indicating large contribution from particles size and shape dispersions which is consistence with the morphological features discussed in the previous section.

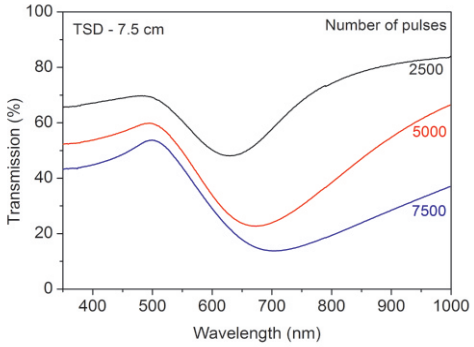

Fig. T.1.7: Optical transmission spectra of the Au films grown with different number of ablation pulses

As mentioned above that the substrate temperature controls the growth mode of the film (either continuous or nanoparticle) thereby plays a strong role for producing films possessing strong LSPR response. Fig. T.1.8 compares the transmission spectra of the Au films grown at different substrate temperatures i.e. RT, 150˚C, 300˚C and 500˚C with 5000 number of ablation pulses.

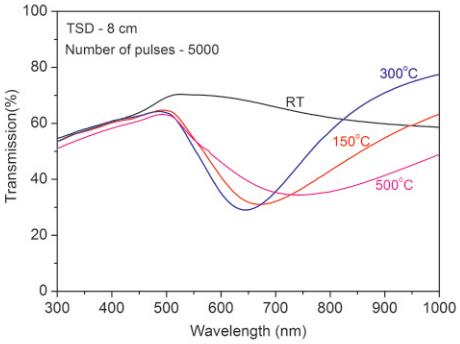

Fig. T.1.8: Optical transmission spectra of the Au films grown at different substrate temperatures

It may be noted that for a continuous film, the free electron response spreads over a wide wavelength range and produces monotonously decreasing transmission with the wavelength. However for nanoparticle films, the LSPR excitation confines the oscillator strength to a narrow band where the transmission becomes low and further it increases with the wavelength unlike that of a continuous film. The figure depicts that for the same mass thickness of the films, those grown at higher substrate temperatures have shown a

significant dip in the transmission whereas that produced at RT has shown nearly constant or monotonously decreasing transmission resembling to the response of a percolated or thin continuous metal film. The substrate temperature of about 300°C was found to be the optimum temperature for producing strong LSPR response.

Without much alteration of the morphology of the film, it is also possible to realize LSPR wavelength tuning by variation of frequency dependent dielectric function of the metal as a consequence of Frohlic condition mentioned above. In view of this, alloy nanoparticles are being explored as novel plasmonic materials for different applications. Bimetallic Ag-Au and Ag-Cu nanoparticle films of different compositions and thicknesses were grown using sequential pulsed laser ablation where the film composition was tuned by varying the ratio of number of ablation pulses of Ag and Au/Cu [6, 7]. Using X-ray photoelectron spectroscopy and energy dispersive spectroscopy, Ag-Au alloy formation and composition of the metals was determined. Fig.T.1.9 shows the transmission spectra of Ag-Au alloy nanoparticle films. With the variation of the film composition, the LSPR wavelength tuning in the range of 450-700 nm was achieved for Ag-Au alloy system [6]. For Ag-Cu bimetallic films with help of alumina capping layer, the LSPR wavelength tunable films stable in the atmospheric condition were also produced [7].

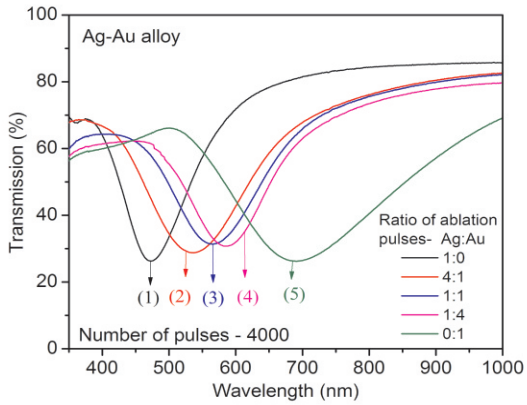

Fig. T.1.9: Optical transmission spectra of the Ag-Au alloy nanoparticle films of different compositions

We have also studied the LSPR responses of Ag films grown under different process parameters of PLD including gas ambience [8]. It was observed that though Ag has strong LSPR response compared to Au, it readily forms oxides in atmospheric ambient and thus shows atmospheric tarnishing of its LSPR characteristics. In order to circumvent this problem, Ag films of different thicknesses with alumina (dielectric) capping layers were grown and their LSPR characteristics and stability in ambient conditions were investigated [9]. It was observed that for uncapped nanoparticle films of lower mass thickness the LSPR response disappeared in about 2-3 months while those of higher mass thickness films degradation of LSPR response with time was noticed as shown in Fig. T.1.10. In contrast to this, the alumina capped Ag nanoparticle films of both the thicknesses retained their SPR response over four months of observation.

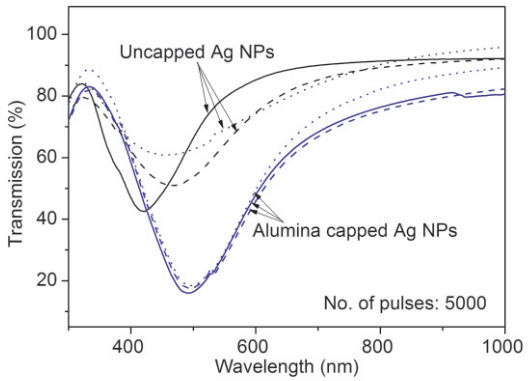

Fig. T.1.10: Transmission spectra of uncapped and alumina capped Ag nanoparticle films after, deposition (Solid), two months (dashed) and four months (dotted).

The dielectric capping layer not only protects the films against atmospheric tarnishing but also influences the LSPR response of PMNPs films due to change in surrounding dielectric constant. Fig.T.1.11 shows the transmission spectra of Au films capped with alumina layer grown with same parameters as shown in Fig. T.1.8. It can be observed that after alumina capping, the transmission slightly increased at lower wavelengths and decreased at higher wavelengths (> 500 nm) along with red-shifted LSPR band. Increased transmission in the inter-band absorption region is because of re-sputtering of the Au films which is relatively higher for the films grown at low TSD [5].

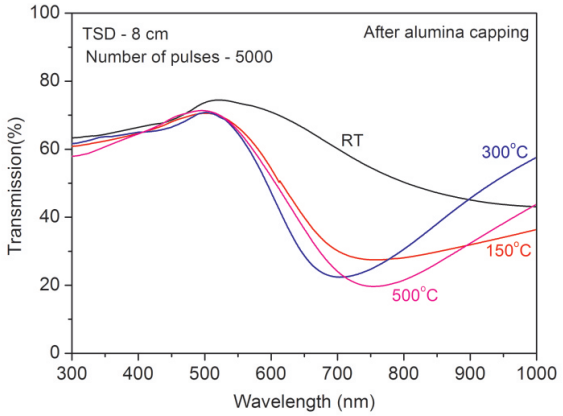

Fig. T.1.11: Optical transmission spectra of the Au films along with alumina capping layer deposited at different growth temperatures

PMNPs films with gradually varying LSPR characteristics offer understanding the role of plasmonic effects in systematic and simplified approach which can be achieved through gradient mass thickness [10]. As mentioned above that in PLD, the deposition is highly directional as a result it allows growth of gradient thickness films depending on TSD and substrate size [11]. Fig.T.1.12(a) presents the transmission spectra of Au films of gradient thickness deposited at 4.5 cm TSD with 5000 pulses at RT and 300°C and the inset shows the photograph of the sample (grown at RT) indicating the positions of the recorded spectra. Scanning electron microscopic (SEM) images of the films grown at 300°C on GaAs substrate reveals that the mean size of the particles reduced significantly from the region-I to III as shown in Fig. T.1.12(b, c). Other than these parametric variations, the laser fluence and the effect of gas ambience on the formation of PMNPs growth in PLD was also studied [4, 12].

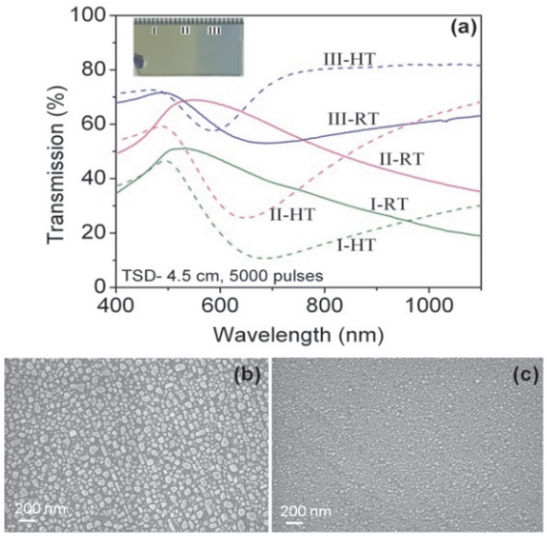

Fig. T.1.12: (a) Optical transmission spectra of gradient thickness Au films grown at RT (solid lines, with photograph) and 300°C (dashed lines), SEM image of region-I (b) and region-III (c).

2.3 Theoretical aspects

As shown above, the optical response of PMNPs films strongly depends on their morphological features, particle density and substrate on which they were deposited. With known dielectric function of metal/alloy, the optical response of PMNPs on a substrate can be calculated using a suitable effective medium theory predicted dielectric function (ε_{eff}) considering the effects of substrate. For PMNPs on a substrate, Yamaguchi effective medium model is appropriate since it includes the substrate dipole image effects on the optical response of these nanoparticles. From the Yamaguchi's model, the effective dielectric function (ε_{eff}) of the system is given by:

$$\varepsilon_{eff} = \varepsilon_m \left(q \frac{\varepsilon(\omega) - \varepsilon_m}{\varepsilon_m + F(\varepsilon(\omega) - \varepsilon_m)} + 1 \right)$$

where, ε_m is the dielectric function of the surrounding medium, $\varepsilon(\omega)$ is the dielectric function of the particle, q is the metal volume filling fraction and F is the total depolarization factor contributed by the different shape and configuration factors of MNPs supported on substrates [13]. One of the limitations of this model was the low coverage limit i.e. only applicable where the separation between the particles is large compared with their size. Also as the shape of a fixed-volume particle deviates from that of a sphere, the distance between the centre of the particle and its image dipole decreases. This leads to a rapid increase in the additional field from the image charge, causing discontinuity in F for spheroidal particles in the Yamaguchi model. Fedotov et al modified the Yamaguchi model which overcomes the above limitations [13]. According to this model, the effective depolarization factor has been modified for spherical as well as spheroidal particles of all aspect ratios and is also applicable to large metal volume filling fractions even close to one. We have studied the Ag-Au alloy dielectric function obtained from three different analytical models and the LSPR response was calculated using the modified Yamaguchi model [6]. Fig. T.1.13 presents the theoretically predicted LSPR wavelength with the alloy composition and metal (Ag-Au alloy) volume filling fraction in the film for the particles with aspect ratio ~ 3. The figure depicts that for any given metal composition, increasing metal volume filling fraction resulted into red-shifted LSPR due to increased interactions between the particles and with the substrate. Also for the entire observed LSPR wavelength range shown earlier, the theory predicts high package density of the nanoparticles which is consistent with the AFM analysis.

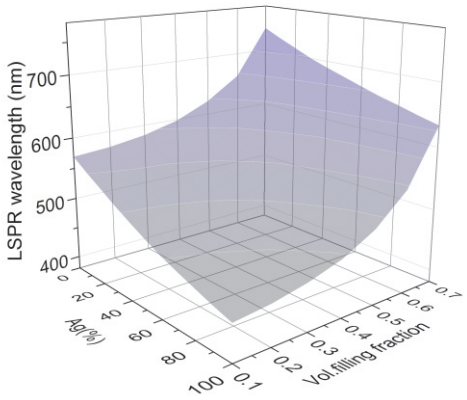

Fig. T.1.13: Variation of LSPR wavelength of Ag-Au alloy PMNPs films with Ag(%) and volume filling fraction

2.4 SERS responses of Au nanoparticle films

As observed above, all the PLD grown films are densely packed which produce large number of hot spots, highly attractive for surface enhanced Raman scattering (SERS) based sensing applications. The SERS response of probe molecules in presence of PMNPs is affected by various parameters such as metal nanoparticle size, inter-particle spacing, hot spot density, excitation wavelength etc. Fig.T.1.14 presents the SERS response of Au films grown at different growth temperatures using Rh6G dye as probe. The figure shows that the film grown with high substrate temperatures have produced strong SERS response which is in line with the observed LSPR response of these films. Among different densely packed nanoparticles films of same mass thickness produced at different growth temperatures, the films with high LSPR strength near the excitation wavelength was found to be highly suitable for SERS sensing [5].

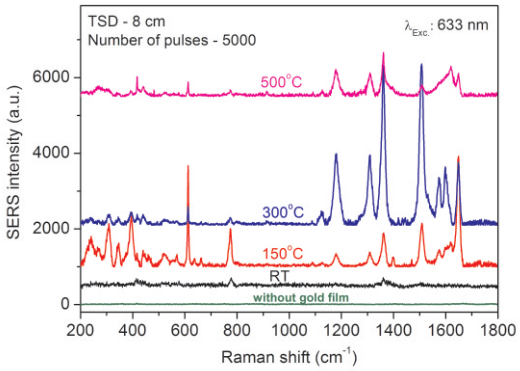

Fig. T.1.14: Variation of SERS intensity of Rh6G dye in presence of Au films grown at different substrate temperatures

3. LPPLA grown colloidal nanoparticles

LPPLA process is one of the promising top-down methods for the single step growth of plasmonic metal nanoparticles in different solvents with and without capping agents which provide stability to the nanoparticles. Unlike chemical reduction based nanoparticles synthesis methods, the LPPLA method is less sensitive from the concentration of capping agents because laser ablation mainly depends on the optical and thermal properties of the target and liquid. In this process, the pulsed laser beam ablates the metal target inside the liquid medium which confines the produced metal vapour and molten droplets grow into nanoparticles. Using third harmonic Nd:YAG laser as shown in the experimental setup (Fig. T.1.15), Au nanoparticles (NPs) were produced by ablating the Au target for 15 min in ultra-pure water. The Au NPs solutions were found to be stable against aggregation, which is attributed to the negative surface charge on the particles. Because of this, these nanoparticles show electrostatic interaction with cationic dyes like Rhodamine6G and change the photo-absorption and photo-luminescence (PL) of Rh6G. Using these effects, these composite systems are being used in different applications like detection of carcinogenic species, nano-scale spectroscopic ruler, random lasing etc.

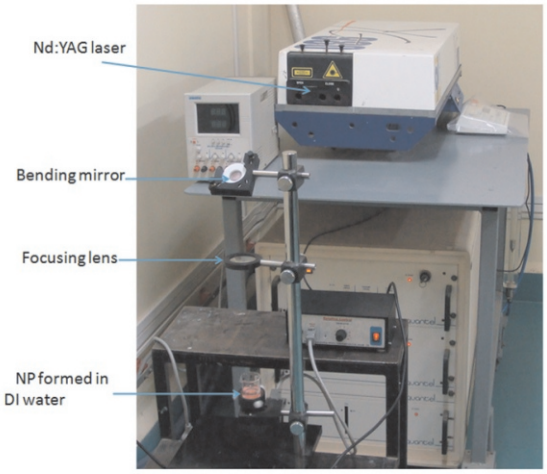

Fig. T.1.15: Liquid phase pulsed laser ablation experimental setup at our laboratory

Figs. T.1.16(a) and T.1.16(b) show the transmission electron microscopic (TEM) image of LPPLA grown AuNPs and absorbance spectra of the composites with different concentrations of Rh6G respectively. The additional absorbance peak observed in the composites is due to dye induced aggregation of AuNPs which generates very large hot spot density useful for different applications [14, 15].

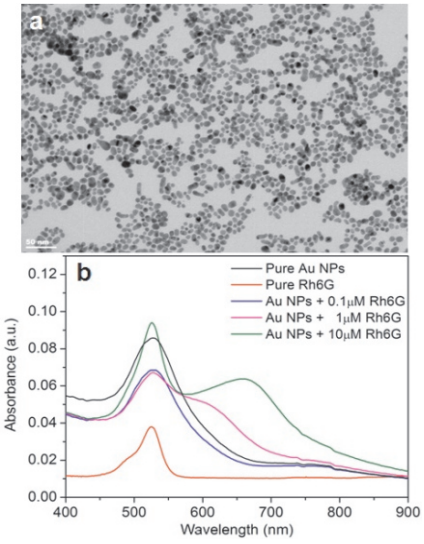

Fig. T.1.16: TEM image of Au nanoparticles in water (a), Absorption spectra of Au-Rh6G composites of different concentrations (b).

Fig. T.1.17 compares the steady state fluorescence of Rh6G dye with and without AuNPs. The quenching in the fluorescence even after inner-filters effect corrections was found to be due to Förster resonance energy transfer (FRET) which is due to significant overlap of LSPR band of AuNPs with the emission band of Rh6G. This non-radiative energy transfer was confirmed from measurements of life time of Rh6G dye using time-resolved fluorescence spectroscopy as shown in the inset of the Fig.T.1.17. A more detailed study on the inter-dependent optical properties of this composite system was also carried out and it was found that concentration of the composites play a vital role on the interaction [15].

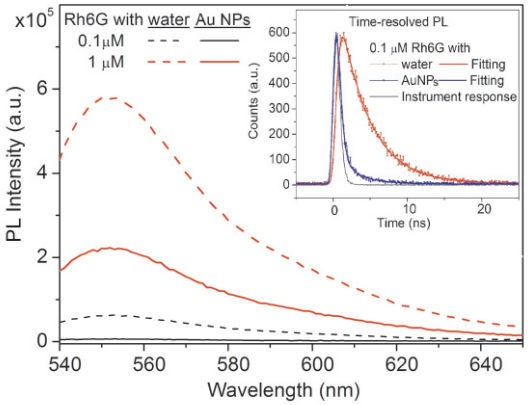

Fig. T.1.17: Steady state fluorescence of Rh6G dye with and without Au NPs, Inset: Life time of the dye measured from time-resolved fluorescence.

We have also addressed the effect of number of laser ablation pulses, type of liquid media and concentration of capping agents on plasmonic properties of LPPLA grown Ag NPs. The NPs were synthesized using the Q-switched Nd:YAG laser (wavelength: 532 nm) ablation of high purity Ag target in different liquids e.g. pure de-ionized (DI) water and solutions with capping agents like: tri-sodium citrate (SC) and sodium dodecylsulphate (SDS) etc. Fig. T.1.18 (a) shows the TEM image of the grown Ag NPs in DI water. Fig. T.1.18 (b) presents the optical absorbance of the Ag NPs grown at different ablation periods. All the grown Ag NPs solutions showed distinct absorption peak at about 400 nm wavelength indicating their LSPR excitation. For the Ag NPs grown in pure water, the maximum absorbance initially increased with the ablation time and then decreased along with increased absorption at longer wavelength region. However those grown in the solutions with high concentration of capping agents, the absorbance monotonously increased with the ablation time, as shown in the inset of Fig. T.1.18(b). Also for a given ablation time, the maximum absorbance was strongly influenced by the nature and concentration of the capping agents.

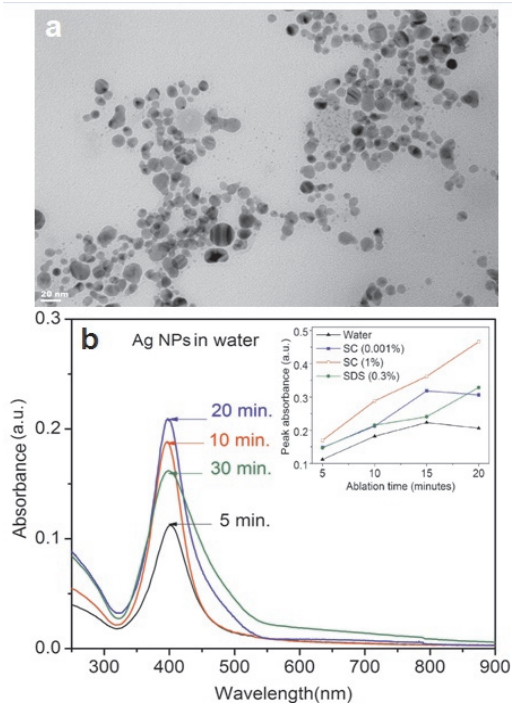

Fig. T.1.18: TEM image of Ag NPs in water (a) Optical absorption spectra of LPPLA grown Ag NPs in water (b) and inset: variation of peak absorbance with ablation time for different liquids.

Ageing effect of Ag NPs in various liquid media was also studied and it was observed that the NPs synthesised in sodium citrate solution are highly stable due to the repulsive force provided by the electric charge double layer. The role of solution pH on the characteristics of this charged layer was also studied [16]. Fig. T.1.19 presents that absorbance of Ag NPs synthesised with 20 min ablation time in different pH conditions of 4 mM sodium citrate solution and also in pure deionised water. Form this figure it can be observed that the pH of the sodium citrate solution has a significant role on the absorbance of Ag NPs grown in LPPLA method. For the solutions with pH $\leq$ 3, laser irradiation did not produce NPs exhibiting significant LSPR absorption peak and also within few minutes the colour of the solutions changed from pale yellow to milky white. But with increasing pH, all the solutions showed LSPR absorption which systematically increased with the pH of the solutions. Particularly at low pH, citrate molecules do not provide charge stability to the formed nanoparticles and also presence of more number of chloride ions readily reacts with the Ag NPs which could be responsible for the change in colour of the solution. It is also important to note that at higher pH conditions the LPPLA grown Ag NPs have shown higher absorbance in comparison to that of reported with citrate capped nanoparticles grown by chemical reduction method. Therefore at optimum processing

parameters, the LPPLA method can be better for producing plasmonic nanoparticles of desired concentrations just by increasing the laser irradiation time.

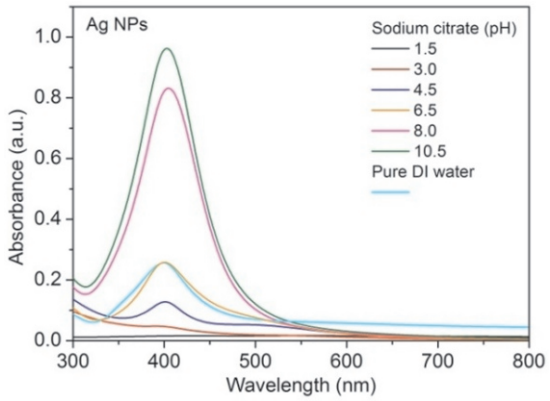

Fig. T.1.19: Optical absorbance spectra of LPPLA grown Ag NPs at different pH values of 4mM sodium citrate solution and also in pure deionised water

4. Conclusion

Plasmonic metal nanoparticles on different substrates as well as in different liquid media were grown by ablating the metal targets using nanosecond pulsed excimer and Nd:YAG lasers. For the first time we demonstrated synthesis of Ag-Au plasmonic alloy nanoparticles with strong LSPR response using sequential laser ablation of different targets. We successfully produced the PMNPs films of controlled LSPR response whose wavelength was tuned in the range of 450 to 750 nm. The role of dielectric capping layer on atmospheric tarnishing and also on LSPR wavelength tuning was addressed for different metals and their alloy nanoparticle films. Theoretical calculations were carried out to predict the LSPR wavelengths of densely packed PMNPs films using modified Yamaguchi model incorporating particle-substrate and particle-particle interactions. The role of LSPR characteristics and film's morphology on surface enhanced Raman scattering of Rh6G dye at nanomolar concentration was determined. Also using liquid phase pulsed laser ablation technique, highly stable colloidal Au and Ag nanoparticles were successfully grown in different liquid media and effects of capping ligands, their concentration and pH on LSPR absorbance have been addressed. With these experimental studies we have shown that pulsed laser ablation methodology is promising to produce metal nanoparticles with high degree of control on their plasmonic characteristics.

Acknowledgements:

The authors acknowledge the characterization support from Dr. A.K. Srivastava, Shri M.K. Singh, Dr. S.K. Rai, Shri H.S. Patel, Ms. S. Bhartiya of RRCAT and Dr. V. Ganesan, Dr. V. Sathe and Dr. D.M. Phase of UGC IUC, Indore. The authors are also thankful to divisional colleagues for their help in the experiments.

References:

1. Ren-Min Ma, R.F. Oulton, V.J. Sorger, X. Zhang, Laser Photonics Rev. 7, No. 1, 1–21 (2013).
2. H.A. Atwater, A. Polman, *Nature Mater.,* 9,205 (2010).
3. S. Maier, Plasmonics: Fundamentals and Applications, Springer-Verlag US (2007).
4. S. Verma, B.T. Rao, S. Rai, V. Ganesan, L.M. Kukreja, Appl.Surf. Sci. 258, 4898 (2012).
5. S. Verma, B.T. Rao, S. Bhartiya, V. Sathe, L.M. Kukreja, Appl. Surf. Sci. 346, 379 (2015).
6. S. Verma et al, J. Appl. Phy. 117, 133105 (2015).
7. S. Verma, B.T. Rao, T. Thakur, S. Bhartiya, L.M. Kukreja, Proc. National Laser Symposium-23, S.V. University, Tirupati (2014).
8. B.T. Rao, S. Verma, M. Gangrade, V. Ganesan, L.M. Kukreja, J. Nanoscience Lett. 3:17(2013).
9. S.Verma, B.T. Rao, D. Reynolds, V. Ganesan, L.M. Kukreja, Proc. Pulsed Laser Deposition of Thin Films and Nanostructured Materials, IIT Kharagpur (2013).
10. T W H Oates and S Noda, Appl. Phys. Lett. 94, 053106 (2009).
11. B.T. Rao, S. Verma, R. Singh, S.K. Rai, L.M. Kukreja, Proc. Pulsed Laser Deposition of Thin Films and Nanostructured Materials, IIT Kharagpur (2013).
12. L.M. Kukreja, S. Verma, D.A. Pathrose, B.T. Rao J. Phys.D:Appl. Phys. 47, 034015 (2014).
13. V.A. Fedotov et al , J. Opt.A: Pure Appl. Opt. 6, 155 (2004).
14. S.Verma et al, presented in International Symposium on Materials Chemistry, BARC, Mumbai (2012).
15. S. Verma, et al. J. Lumin. 155, 156 (2014).
16. B. T. Rao et al, Proc. National Laser Symposium-23, S.V. University, Tirupati (2014).